Polymer 51 (2010) 3582–3589

Contents lists available at ScienceDirect

Polymer

journal homepage: www.elsevier.com/locate/polymer

Structural properties of hydrophilic polymeric chains bearing covalently–linked hydrophobic substituents: Exploring the effects of chain length, fractional loading and hydrophobic interaction strength with coarse grained potentials and Monte Carlo simulations

Massimo Mella [a,b,*], Lorella Izzo [c]

[a] Dipartimento di Scienze Chimiche ed Ambientali, Universitá degli Studi dell'Insubria, via Lucini 3, 22100 Como, Italy
[b] School of Chemistry, Cardiff University, Main Building, Park Place, Cardiff CF10 3AT, United Kingdom
[c] Dipartimento di Chimica, Universitá degli Studi di Salerno, via Ponte Don Melillo, 84084 Fisciano (SA), Italy

ARTICLE INFO

Article history:
Received 12 March 2010
Received in revised form
10 May 2010
Accepted 10 May 2010
Available online 24 May 2010

Keywords:
Polymers
Hydrophobic substituents
Monte Carlo simulations

ABSTRACT

Chemical and physical properties of polymeric species in solution strongly depend on their structure, which can be modulated by covalently linking substituents of different solubility. In this work, the effect of changing the interaction strength and fractional loading of hydrophobic substituents on semi-flexible hydrophilic polymers of varying chain length is studied by means of Monte Carlo simulations and coarse grained model potentials. The latter are chosen in order to provide a more factual representation of a chain in diluted solution, introducing substituent flexibility and realistic torsional and bending potentials. Upon increasing the number and the interaction strength of the substituents, our results indicate a less steep rise of the chain gyration radius and "end to end" distance for the chain length than predicted for an unsubstituted polymer in an almost good solvent. Moreover, a "disordered to compact" structural transition appears. In parallel, the formation of hydrophobic nuclei and the consequent appearance of flexible polymer loops grafted to the semi-rigid cores is witnessed. The core formation resembles a nucleation phenomenon, where the change in the interaction between the substituents modulates the free energy surface for the aggregation process similarly to the change in chemical potential. Interestingly, it has been found that a single chain containing a sufficiently high number of interacting substituents may give rise to the formation of multiple cores, suggesting that the chain stiffness may play a role in defining the structure of the free energy minimum.

1. Introduction

Polymers conjugated to small molecules (e.g. drugs and markers) have been widely studied for different applications, particularly in the biomedical field. The structure of an polymer conjugate comprises a minimum of three components: an polymeric backbone, a linker, and one or more types of molecules with different activities such as antitumor agents, fluorescent dyes or agents for imaging in live cells, targeting moieties, and so on [1–5]. In this context, the conjugation of small molecules to an polymeric carrier can assure many advantages. For example, the action of polymer-drug conjugates is due principally to a prolonged plasma circulation of polymer-conjugates with respect to the free drug and can lead to significant passive tumor targeting by the enhanced permeability and retention (EPR) effect [6]. This allows lower side effects, better pharmacological efficiency of drugs, and less frequent administration. Also, anatomical or molecular information can be obtained by medical imaging [7] with polymer-conjugates to fluorescent dyes or to PET, CT, and MRI imaging agents [8–11].

The protection of the molecules during the plasma circulation until the polymer conjugate accumulates into the target site is one of the fundamental requirements for these entities to work properly. In this respect, attention has been paid to the design of appropriate linkers, whereas the physical chemistry of these species has less frequently been considered. The latter, however, is of high importance due to the different nature of constituents (hydrophilic or amphyphylic for the polymeric carrier and usually hydrophobic for the linked molecules), which can markedly affect

* Corresponding author. School of Chemistry, Cardiff University, Main Building, Park Place, Cardiff CF10 3AT, United Kingdom.
E-mail addresses: mellam@cardiff.ac.uk, massimo.mella@uninsubria.it (M. Mella), lizzo@unisa.it (L. Izzo).

0032-3861/$ – see front matter © 2010 Elsevier Ltd. All rights reserved.
doi:10.1016/j.polymer.2010.05.013

the solubility and the solution behaviour (e.g. the structure) of the conjugate in a way that depends on substituent hydrophobicity and loading. In the final instance, the behaviour of the conjugate in solution is expected to have a bearing on the protection or exposure of the molecules during their transport and action.

The relevance of the physical chemistry of a conjugate to the biomedical field has become clear with the demonstration that the attachment of hydrophobic drugs to hydrophilic carriers can lead to the formation of intra- or inter-molecular aggregates in aqueous solution, which may negatively correlate with the biodistribution, potential toxicity and anti-tumor activity of the polymer-drug conjugate. For instance, we mention the case of the hydrophilic N-(2-hydroxypropyl)methacrylamide (HPMA) cooligomer/amino-ellipticine conjugate, which may form unimolecular micelles as confirmed by measuring pyrene entrapment [12,13] and for which increasing drug loading decreases the drug rate of liberation induced by lysosomal thiol-dependent proteases due to a different accessibility afforded by the intracellular enzyme to the biodegradable polymer-drug linker [12–14]. Similarly, the solution behavior of fluorescent dye/polymeric carrier conjugates have to be considered. These systems are of critical importance in the study of the mechanism underlying drug delivery by polymers to cellular and subcellular targets and, thus, for the design of more effective polymeric drug carriers. Even in this case, the dye loading is expected to be a very crucial factor because it can influence the polymer conformation in solution, and thus its uptake, aggregation, the self-quenching of dye molecules and the formation of excimers and exciplexes [15].

Considering the examples proposed, it should be apparent how the study and, hopefully, the prediction of the physicochemical properties in aqueous solution of these new multifunctional entities are of fundamental importance in order to design and reach an optimal biological rationale. In fact, the influence of one structural component on the performance of the others should be carefully considered to ensure synergy in the integrated design. This notwithstanding, studies in this direction have only rarely been reported [16–23] perhaps due to the technical difficulties encountered in interpreting the experimental results in term of atomistic details. In this context, theoretical methods may cast light on the main features of polymer-conjugates and thus provide insights on the relationship between structure and composition (e.g. a specific degree of polymer folding, micelles formation and the thermodynamics of chain collapse upon hydrophobic substitution [24,25]. Despite the potential to provide a prompt and high quality feedback for the design of new species, the vast majority of theoretical studies on polymers have, however, employed extremely simplified models. For instance, poly-peptides containing hydrophobic residues are often modeled as semi-rigid necklaces of Lennard–Jones beads [24–27] or as chains of non-overlapping lattice sites [25] with highly ordered substituent distribution, thus neglecting some of the important features possessed by substituted polymer-conjugates. For instance, it is expected to be necessary to describe the entropic contribution to the conjugate free energy due to the flexibility of the hydrophobic molecule-linker unit (the pendant) since its magnitude, of order *RT* per pendant, may be sufficiently high to influence the three dimensional structure of the species. Besides, previous studies have only investigated the behaviour of species containing a high fraction (0.5–0.8) of regularly spaced hydrophobic substituents, whereas polymers conjugated usually present a lower content of hydrophobic moieties tethered to the polymeric chain in random locations. In our view, these peculiarities are likely to induce a different solution behaviour and must therefore be taken into account (*vide infra* for our approach to tackle this task, which also includes using a more realistic chain model with bending, torsional and long range interactions). That is of course valid whenever a more accurate, and hopefully more predictive, modeling of the aforementioned polymer-conjugates is sought.

With these ideas in mind, we decided to investigate model polymer-hydrophobic molecule conjugates in order to explore what additional structural features, if any, may emerge from the inclusion of the aforementioned characteristics. In this respect, the aim that we embrace is the exploration of the dependence of the three dimensional (3D-)structure (radius of gyration, hydrodynamic radius, degree of non-sphericity, relative substituent structure, etc) of water soluble model polymers on the substituent interaction strength and on the degree of conjugation (the number fraction of hydrophobic substituents with respect to the monomer units in the polymer). Fig. 1 provides a pictorial representation of this task, highlighting some of the key features in our model and approach.

The organization of this Manuscript is as follow. In Section 2, we introduce the quantitative details of the model chosen to simulate an polymer conjugate and the methodology employed for the simulations. Section 3 presents the results of our simulations, together with a discussion of a few peculiarities that characterize the structural behaviour of our model conjugates. Finally, Section 4 presents our conclusions as well as future avenues of exploration.

2. Theoretical methods and simulations

2.1. Model potentials

With the intention of drawing conclusions of a general semi-quantitative nature for our target systems, we decided to employ a realistic—albeit simplified for computational purposes—description of their effective potential energy surface. As discussed in the Introduction, it is our view that such a model must contain specific ingredients such as the semi–flexible nature of a chain (i.e. stretching, bending and torsional potentials), a realistic description of long range interactions in the appropriate thermodynamics state (monomer interaction mediated by solvent and perhaps counterions), as well as the possibility of tuning the interaction forces between hydrophobic substituents (HPS's). To this end, we have selected to use for the description of the backbone chain the coarse grained model developed by Reith et al. [28] for the sodium salt of poly-acrylic acid (PAA) chains at 333.15 K. This model provides one with a computationally efficient description of the free energy surface for an polymeric chain and it appears suitable for our purposes. In fact, the original model treats the polyanion as a chain of beads centered on the center of mass of the monomers, which are linked by harmonic springs and subjected to numerical bending, torsional and long distance potentials parameterized using atomistic molecular dynamics simulations. The latter two components provide a reasonably general representation for the monomer excluded volume and for the hindrance expected to local conformational changes in an polymeric chain in an almost good solvent (*vide infra*), which is the situation one is confronted with when the unsubstituted polymers mentioned in the Introduction are concerned. In this respect, it is worth mentioning that the interaction between non-linked monomers is only weakly binding at distances larger than 8 Å (at the minimum, the value of the potential is roughly 0.016 kcal/mol at 333.15 K ≡ 0.66 kcal/mol), whereas it is more strongly repulsive in nature at shorter distances. It therefore represents mainly the monomer excluded volume.

Given our intention of modeling the general properties of a class of systems, we describe the interaction between HPS's using a pair sum $V(\mathbf{R}) = \sum_{i<j} U(r_{ij})$. In this work, the simplified description provided by a square well potential of the form.

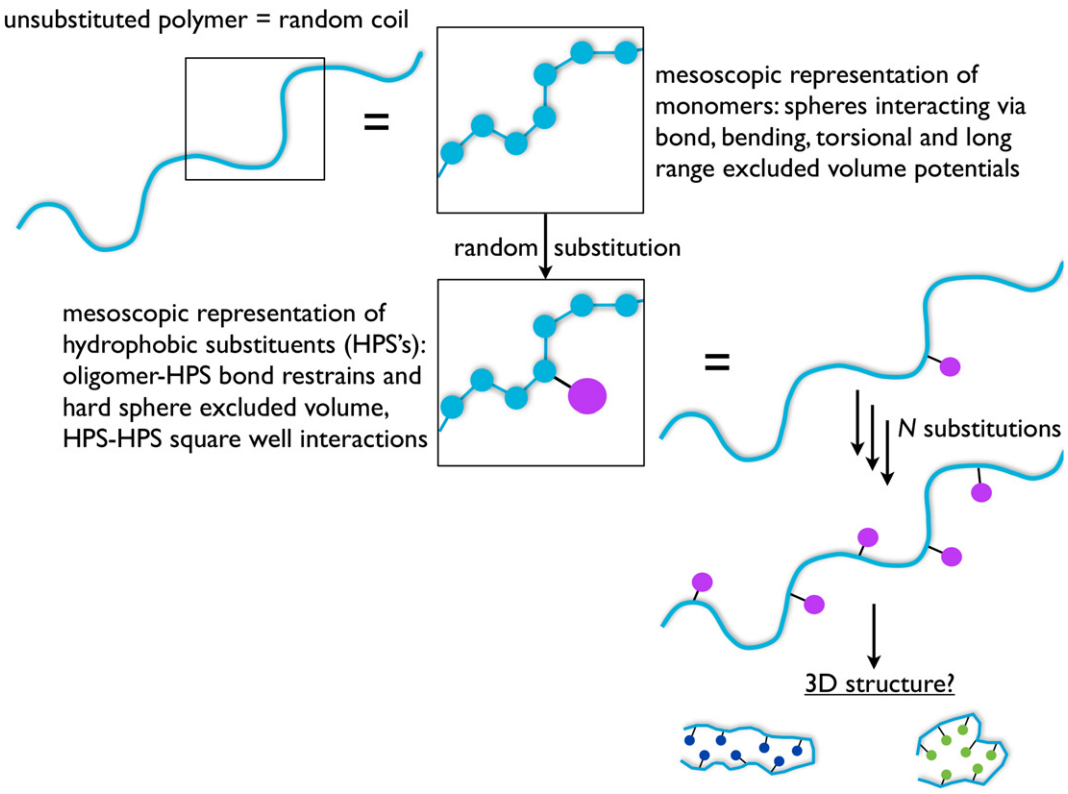

Fig. 1. Scheme representing the modeling approach employed to study the dependence of the structural features of polymer-hydrophobic substituent conjugates on the number (N) and interaction strength of the hydrophobic pendants. The latter are represented with different colors to indicate a different magnitude for the inter-substituent interaction.

$$U(r) = \begin{cases} \infty & (r \le s) \\ -V_0 & (s < r \le s + \delta) \\ 0 & r > s + \delta \end{cases} \quad (1)$$

was used for the pair potential, with the parameters $V_0 \ge 0$, $s = 3.7$ Å and $\delta = 5.0$ Å being chosen in order to represent the effective (i.e. containing also the effect of the solvent molecules) forces between HPS couples. While hydrophobic forces should, in principle, depend on the density of interacting pairs due to excluded volume effects, the simplified model chosen in this work is expected to provide a sufficiently accurate representation for these forces and guidance to understand general trends, and it is in line with the spirit of the pairwise coarse grained potential employed to model the polymeric chains. Besides, the deepest well of the potential of mean force for two hydrophobic species in aqueous solution is better modeled with a function that assumes zero interaction energy at a finite distance.

To investigate the dependence of the system properties on the strength of the hydrophobic forces, several values for V_0 were used in our simulations (*vide infra*). Guidance in choosing the set of values for V_0 was obtained from previous studies where the potential of mean force between hydrophobic species in water was studied using molecular simulations [29–35]

To model the flexible spatial orientation of pendants tethered to an polymer, substituents were linked to the chains using the harmonic restraining potential $U_b(r) = 1/2k(r - r_0)^2$. Here, r is the distance between the center of mass of the HPS and of the linked monomer, $r_0 = 4.20$ Å is their equilibrium distance and $k = 1.08$ kcal/(mol Å^2). The interaction between an HPS and non-linked monomers is described using a hard sphere potential, whose repulsive wall onsets at distance s. The location of HPS along a chain was randomly chosen in order to mimic the statistical distribution that is expected from covalently tethering pendants to an polymer; substitutions on neighbor monomers and on the first and last monomers in the polymer where excluded.

2.2. Monte Carlo simulations

As shown by Reith et al. [28] in their original work on the PAA anions, the latter affords a high degree of structural flexibility thanks to the weak interaction between non-linked monomers; in fact, the hydrodynamic radius (R_H) of a chain grows proportionally to $N^{0.55}$ upon increasing the number of monomers N. Such behavior is very close to that of a Gaussian chain in good solvent, a fact that allows the simulation of fairly long polymers using a straightforward adaptation of the canonical Monte Carlo (MC) method [36]. In the latter, local monomer displacements are attempted in Cartesian space using the original MC scheme proposed by Metropolis et al. [36] whereas global torsional moves may be carried out using the approach proposed by Betancourt [37]. In our implementation of the method, monomers attempt a displacement one by one in a systematic fashion using a local and symmetric Metropolis MC move; each attempt is accepted accordingly to the standard rule $P_{acc} = \min [1, \exp(-\Delta V/(kT))]$. Torsional moves were carried out after all monomers have made 10 attempted displacements; the pivot bond around which the rotation takes place and the orientation (clockwise or counter clockwise) are chosen randomly. Even in this case, the distribution of attempted rotations was taken to be uniform and symmetric over an interval of angles centered on the current torsional angle and accepted employing the standard Metropolis rule.

In the case of the substituted systems investigated in this work, the presence of HPS's was however found to induce roughening in the potential energy surface; this was especially true when a large number of substituents (N_s) and high V_0 values were used. Thus, we

fund that straightforward MC simulations became quasi-ergodic or suffered from a serious slowing down in their exploration of the conformational space. As a consequence, a parallel tempering (PT) [38] scheme was therefore implemented and used to limit the impact of these difficulties. In the PT approach, parallel MC simulations were carried out at several temperatures including the target one (T_t = 333.15 K) and configurations from different temperatures, either in the vicinity [38] or randomly chosen over the complete set [39] are swapped with a probability that conserves the correct canonical distributions. Generally, we employed 5–7 equally spaced temperatures between T_t and a T_{max}, with T_{max}being chosen so that the substituted chain was almost unfolded. The number of parallel simulations was chosen in order to have an acceptance probability for the replica swaps between neighbor temperatures of roughly 0.2 when attempted after 100 MC sweeps (one sweep represent the attempted local displacement of all monomers in a chain). In this way, the faster exploration afforded by high temperature simulations is exploited whilst keeping the magnitude of the statistical noise at the target temperature under control. It is also important to stress that, given the nature of the coarse grain potential used to model the chains, we focus our attention on the structural changes in our species as a function of N_s and V_0, and that the usage of the PT scheme is a mere device to facilitate the ergodic exploration of the configurational space.

Depending on the number of monomers in the polymer ($92 \leq N \leq 368$) and on the strength of interaction between HPS pairs ($0 \leq V_0/(k_BT_t) \leq 3.1$), PT simulations have been carried out using 10^6–10^7 MC sweeps per temperature after, at least, 10^6 sweeps of thermalization. Convergence of the average values was tested by monitoring the evolution of partial averages and comparing their fluctuation with the associated standard error. For chains with a very rough energy landscape, it was occasionally necessary to run additional simulations starting from stochastically independent initial geometries in order to check the proper convergence of expectation values. Albeit this approach does not guarantee absolute convergence, it however provides with some additional assurance on the quality of the simulations results. The robustness of the results discussed in the following Sections with respect to the location of the HPS's along the chains was also tested running simulations for a few of species with statistically independent distribution of the substituents.

3. Results and discussion

As indicated in the Introduction, our main interest is to investigate how the structural properties of semi-flexible and soluble chains are modified upon introducing of a limited number of hydrophobic substituents. Albeit we focus on models with sufficiently general properties to represent a wide class of systems, we expect this information to be able to provide some guidance in choosing the maximum load of HPS's (i.e. drug molecules) to avoid a collapse of the polymeric chain onto itself, or, conversely, in selecting appropriate substituents to generate a core-shell structure (i.e. with pendants protected by the polymeric chain).

To remain as parallel as possible to the information on the structural effects of HPS's tethered to soluble chains [23] we restrain ourself to a maximum chain length ($N \leq 368$) and number of substituents ($N_s^{max} \sim 0.1 \times N$) and investigate the change in structural properties of our model systems as function of the fraction $x_s = N_s/N \leq 0.1$. It is important to stress that the upper bounds placed on the number of monomers and pendants are related, respectively, to the polymer length used in drug therapy and to the lower aggregation limit found experimentally for soluble chains conjugated to hydrophobic drug molecules.

Table 1 presents the data obtained while testing our implementation of the potential developed by Reith et al. [28] for a small set of unsubstituted chains (N = 92, 184 and 368); the case N = 92 was chosen to allow for a direct comparison with the data in Ref. [28].

As shown in Table 1, the $\sqrt{\langle R_g^2 \rangle}$ value for N = 92 agrees with the published one Ref. [28] within statistical error, thus indicating the correctness of our routines. The data in Table 1 provide also the basis for a comparison with substituted chains. As for the latter, Figs. 2–4 present the main numerical results of this work, showing the changes in $\sqrt{\langle R_g^2 \rangle}$ as a function of N_s and V_0 for the three chains N = 92, 184 and 368.

Fig. 2 shows a decrease in the gyration radius upon increasing the number of substituents and the strength of their interaction. Despite this similarity, one also notices a few qualitative differences in the behaviour of $\sqrt{\langle R_g^2 \rangle}$ as a function of N_s in the range of V_0 values explored. In particular, we observe that for $x_s < 0.03$ the average gyration radius remains very close to the one for the unsubstituted chains, thus suggesting entropy as the main driving force for the 3-dimensional structure even when strong HPS interactions are present. When $x_s \geq 0.055$, $\sqrt{\langle R_g^2 \rangle}$ appears to decrease substantially upon increasing $V_0/(k_BT)$, with the highest value of x_s (roughly 0.11) presenting indications for a transition from an open structure to a more compact one. In particular, we see that $\sqrt{\langle R_g^2 \rangle}$ for the case N = 368 and x_s = 0.11 appears to have reached a low plateau around $V_0/(k_BT)$ = 2.4, suggesting that the substituted chain has collapsed into the most compact affordable structure within the constraints imposed by the intra-chain potential. Also noteworthy is the fact that the sigmoidal shape of the $\sqrt{\langle R_g^2 \rangle}$ versus V_0 curve closely resembles the one commonly witnessed during a phase change in atomic clusters as a function of $V_0/(k_BT)$ in many structural indicators (e.g. the average inter-particle distance $\langle r_{i,j} \rangle$ or Lindemman index) [40,41].

A different perspective on the results shown in Fig. 2 is provided by Fig. 3, where some of the data are shown as a function of the chain length for fixed $V_0/(k_BT)$ and x_s values.

Albeit over the limited range of N values shown in Fig. 3, the data for the unsubstituted chains follow closely a power-like trend with $\sqrt{\langle R_g^2 \rangle} \sim N^{\alpha}$ as originally found in Ref. [28] Differently, one notices the presence of a substantial change in the behaviour of $\sqrt{\langle R_g^2 \rangle}$ as a function of N when $V_0/(k_BT) > 0$. Whereas, in general, $\sqrt{\langle R_g^2 \rangle}$ deviates from the simple N^{α} form by a degree that depends both on x_s and V_0, we highlight the presence of two interesting deviations. First, one notices a sudden change in $\partial \ln(\sqrt{\langle R_g^2 \rangle})/\partial \ln N$ on going from N = 184 to N = 368 when (x = 0.055;$V_0/(k_BT)$ = 2.8) and (x = 0.11;$V_0/(k_BT)$ = 2.4). In both cases, the slope drops almost to zero which indicates that there may be either a compensating effect between the increase in chain length and the effective intra-chain interaction (i.e. including the thermal energy and the chain stiffness), or that the system has collapsed to a compact state where the fragments of the chain separating pendants need to acquire a 3-dimensional structure that minimizes the average system size. At variance with these two cases, the decrease in $\partial \ln(\sqrt{\langle R_g^2 \rangle})/\partial \ln N$ is somewhat less marked when (x = 0.11;$V_0/(k_BT)$ = 2.8), thus apparently contradicting the expectation of a similar, if not larger, decrease due to a stronger inter-pendants interaction.

Table 1
Average value of the gyration radius $\sqrt{\langle R_g^2 \rangle}$ (in nm) of the unsubstituted PAA anion chains as a function of the chain length $92 \leq N \leq 368$. The standard error is reported between brackets and refers to the last quote digit.

N	$\sqrt{\langle R_g^2 \rangle}$ this work	$\sqrt{\langle R_g^2 \rangle}$ [28]
92	2.9(1)	3.1
184	4.1(1)	
368	5.6(1)	

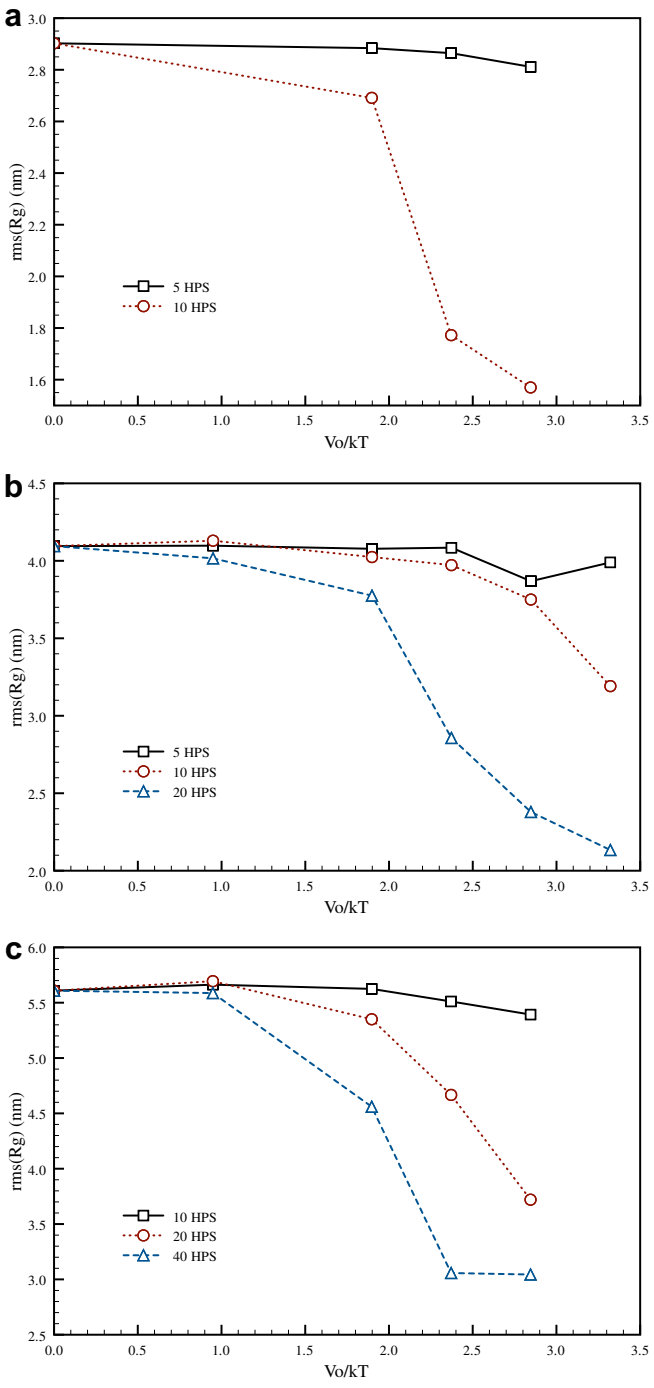

Fig. 2. Dependence of $\sqrt{\langle R_g^2 \rangle}$ (in nm) with respect to the well depth of the hydrophobic substituent interaction (V_0, in units of k_BT). From top to bottom: $N = 92$; $N = 184$; $N = 368$. The number of substituents on each chain is indicated in the three panels as "N_s HPS".

As a first step in shedding some light on the behaviors highlighted in both Figs. 2, 3, Fig. 4 shows the probability distribution function of $\sqrt{\langle R_g^2 \rangle}$ for the case $N = 184$ and $x_s = 0.11$ as a function of $V_0/(k_BT)$. From the distributions shown in Fig. 4, it appears that both the position of the maximum and the width of the distributions decrease in a monotonic fashion upon increasing the value of V_0. In other words, both the average size and the amplitude of the chain fluctuations decrease, indicating that the net effect of increasing

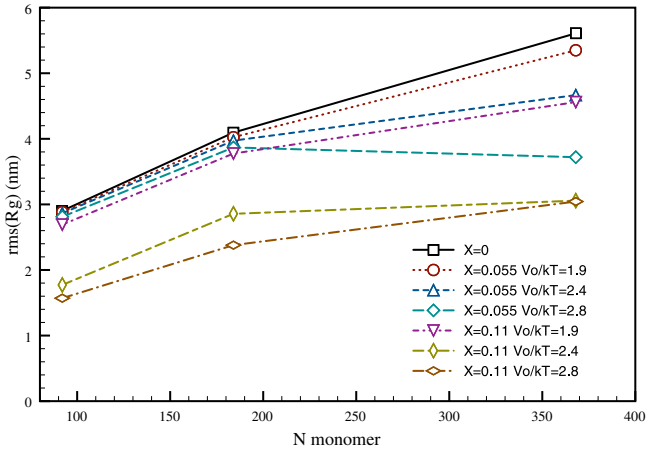

Fig. 3. Dependence of $\sqrt{\langle R_g^2 \rangle}$ (in nm) on the chain length at fixed value of the well depth V_0 (in units of k_BT) and substituent fraction $x_s = N_s/N$.

the substituent interaction is akin to a reduction in the probability of visiting conformations in which the polymer is highly elongated.

Another informative distribution is represented by the probability density of finding any two HPS's at a specific distance r, which is presented in Fig. 5 for the chain with $N = 184$ and $N_s = 20$. The latter shows a substantial reduction in $\sqrt{\langle R_g^2 \rangle}$ as a function of $V_0/(k_BT)$ (see Fig. 2). Upon increasing the value of V_0, it is seen that the distribution evolves from a fairly diffused one at $V_0/(k_BT) = 1.90$, which also presents some indication for a short range structuring of the substituents due to their interaction ($0.37 \leq r \leq 0.87$ nm), to one that shows an increasingly larger amount of neighbor and next-neighbor pairs (the first and second sharp peaks at low distances) together with a broad feature at large r values that evolves from the very diffuse distribution at low value of V_0. Interestingly, the broad feature for the species with $V_0/(k_BT) = 3.31$ has its maximum a longer distance than the one with $V_0/(k_BT) = 2.84$, thus suggesting a more rigid three dimensional structure for the former. Whereas the interpretation of the two peaks at low value of r is unambiguous, the feature around 2.6 nm is difficult to assign to any specific type of structural detail and deserves further attention. To clarify this matter, we have randomly extracted configurations during the MC simulations to visualize a subset of typical chain conformations, some of which are shown in Fig. 6.

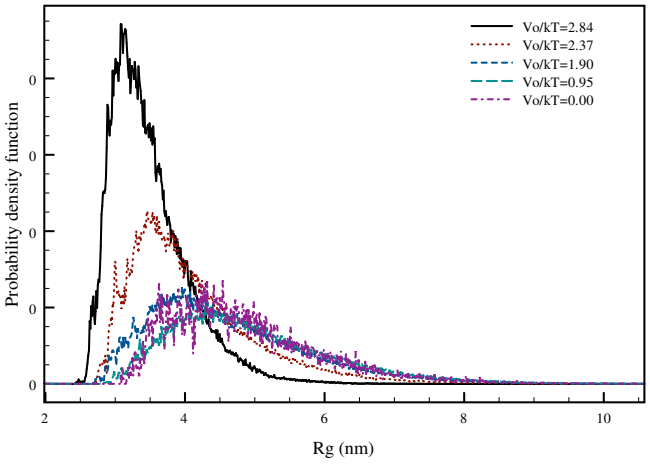

Fig. 4. Probability distribution function for $R_g \equiv \sqrt{\langle R_g^2 \rangle}$ (in nm) obtained simulating a chain containing 368 monomers and 20 substituents ($x_s = 0.055$) at various values of $V_0/(k_BT)$. The distributions $p(R_g)$ is normalized so that $\int dR_g R_g^2 p(R_g) = 1$.

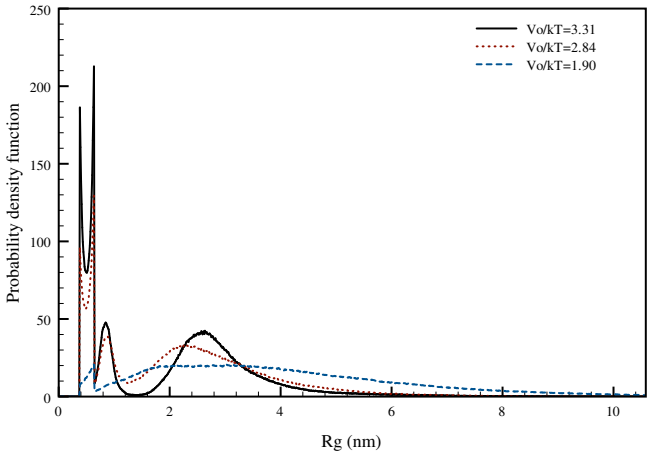

Fig. 5. Probability distribution function for the distance r between two substituents (in nm) obtained simulating the chain containing 184 monomers and 20 substituents ($x_s = 0.11$) at various values of $V_0/(k_BT)$. The distributions $p(r)$ have been normalized so that $\int dr r^2 p(r) = 1$.

From Fig. 6, it becomes evident that the hydrophobic substituents tend to aggregate upon increasing the value of V_0, thus forcing the polymer to produce loops containing varying numbers of monomers in order to accommodate the compact organization of the pendants. Even more interesting is the fact that the species show the tendency of forming two major HPS clusters (nuclei) when $V_0/(k_BT) = 3.31$, each one containing 8–10 pendants. We have also found other instances in which smaller clusters (e.g. 3–4 HPS's) are present, albeit only in the cases of weaker substituent interactions as shown in the top panel of Fig. 6. Apart from the aforementioned loops, the di-nuclear species is also characterized by the fact that the two nuclei are held separated by partially stretched chain segments acting as "spacers".

The peculiarity of the di-nuclear structure shown in Fig. 6 may be appreciated by comparing our findings with the results of simulations carried out on clusters and chains of particles interacting by means of a square well potential similar to the one given in Eq. (1) [41]. At variance with our results, the free energy minimum of both clusters and chains of square well particles appeared to present a closely packed mono-nuclear structure for similar values of $V_0/(k_BT)$. In our view, this difference seems to suggest that the main effect of the polymeric chain is to destabilize configurations that are too tightly packed thanks to both enthalpic and entropic intra-system effects. Whereas the former have their origin in the excluded volume of the substituents and in the intra-chain potential (i.e. stretching, bending, torsional and long range forces), the latter are related to the smaller volume of configurational space that would be available to mono-nuclear species when the vast majority of the HPS's are contained in a single aggregate.

In this context, it would be useful to remember that the results for model lattice proteins containing a high fraction of HPS's have shown that the latter tend to fold forming a single hydrophobic core [42,43] in a similar range of $V_0/(k_BT)$ values. Moreover, the thermodynamical signature of their "coil to compact" structural transition becomes more evident upon increasing N, thus suggesting the global nature of such an event. Given the fact that these lattice models contained a sufficiently high number of hydrophilic monomers acting as spacers between the hydrophobic ones, it seems likely that the di-nuclear structure afforded by our species could be due to the smaller fraction of HPS's.

Retrospectively, the issue raised by the long distance features highlighted in Fig. 5 for the two cases $V_0/(k_BT) = 3.31$ and 2.84 is answered by observing that two clusters are formed when using

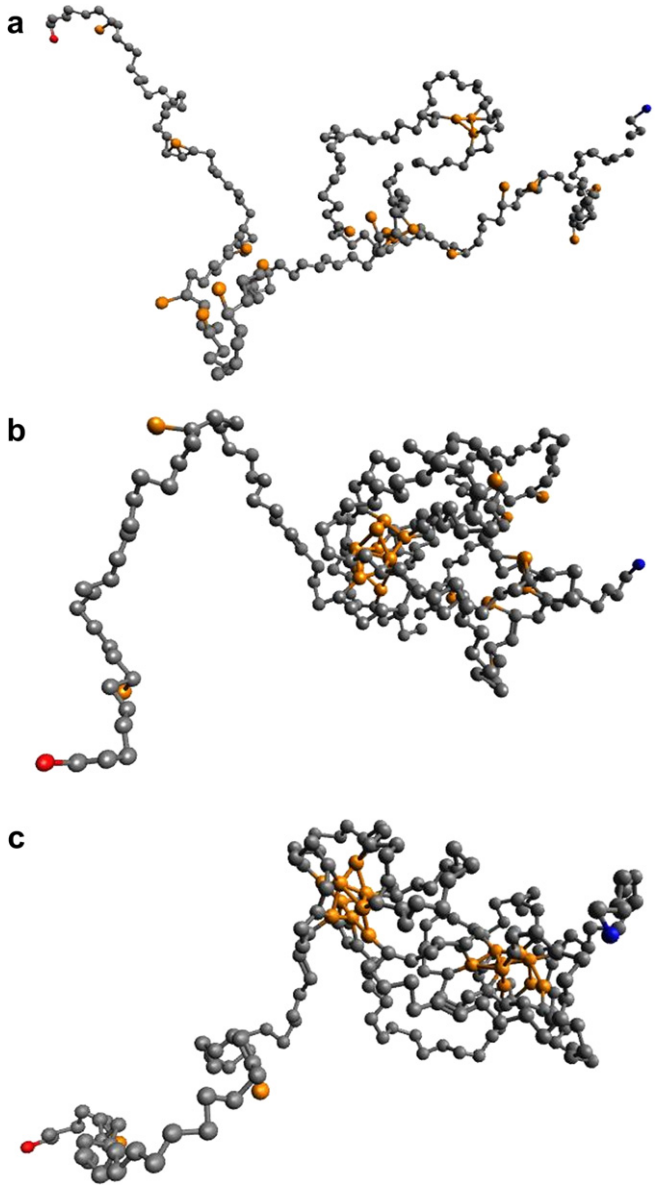

Fig. 6. Sample structures extracted from the simulations of the chain containing $N = 184$ monomers and $N_s = 20$ substituents with $V_0/(k_BT) = 1.90$ (top panel), 2.84 (middle panel) and 3.31 (bottom panel). Light grey spheres represent the chain monomers while orange spheres represent the substituents; blue and red spheres indicate the terminal monomers in the polymer. Notice the incremental formation of a poly-nuclear species upon increasing the hydrophobic interaction potential.

these two interaction strengths; in fact, the long range and broad feature is located at a distance compatible with the inter-nuclear distance as measured from the set of structures collected from the simulations. Also, the broader structure present around 2.2 nm in the simulation with $V_0/(k_BT) = 2.84$ is likely to be due to the reduced number of substituents present in one of the two clusters and to the enhanced chain flexibility that this allows.

Related to the finding just discussed, there is the interesting question of what degree of control one may afford on the formation of poly-nuclear structures such as the one evidenced in Fig. 6. To answer it, Fig. 7 presents two snapshots extracted from simulations carried out using $N = 368$ monomers, $V_0/(k_BT) = 2.84$, and $x_s = 0.055$ or $x_s = 0.11$ (i.e. 20 or 40 pendants). From these images, one evinces that the number of nuclei formed depends on the number of substituents. In fact, the chain containing 40 pendants

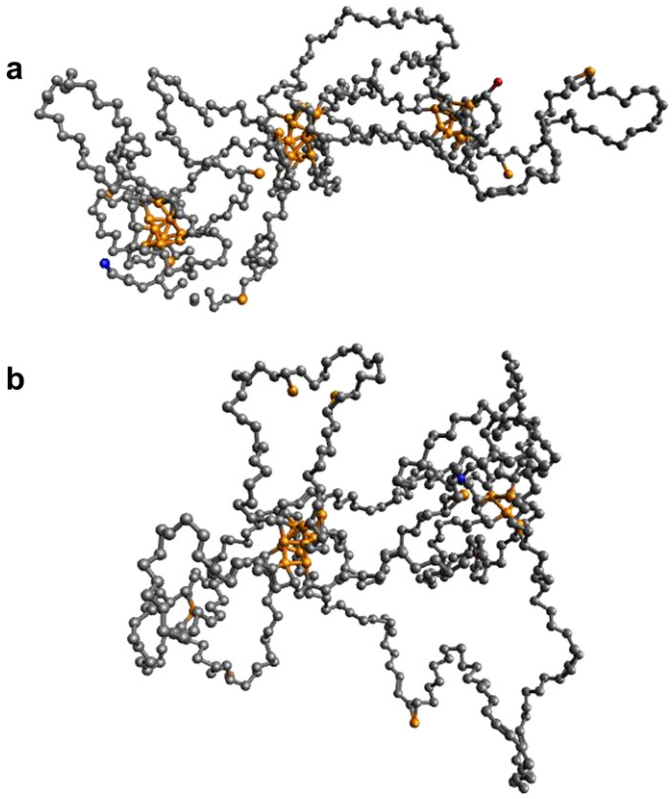

Fig. 7. Sample structures extracted from the simulations of a chain containing $N = 368$ monomers, with $N_s = 40$ (top panel) and $N_s = 20$ (bottom panel) substituents using $V_0/(k_BT) = 2.84$. Grey spheres represent the chain monomers, orange spheres and sticks represent the substituents, whereas blue and red spheres indicate the terminal monomers in the polymer. Notice the increasing number of nuclei and substituent per nucleus upon increasing N_s.

forms 3 almost equi-spaced nuclei, whereas the polymer with $N_s = 20$ forms only two. As a consequence of this difference, the former has shorter loops and "spacers". It is also worth noting the fact that the species with the highest N_s forms clusters that contain, on average, more hydrophobic moieties (roughly 11–12 versus 5–8), thus suggesting that it may be possible to have some control on the size of the nuclei as well.

Incidentally, the structures shown in Fig. 7 also provide an explanation for the different behaviour of $\sqrt{\langle R_g^2 \rangle}$ versus N highlighted (see Fig. 3) for the case $x_s = 0.11$ and $V_0/(k_BT) = 2.84$. In this respect, the increase of the average gyration radius upon going from $N = 184$ to $N = 368$ despite the high value of V_0 and the large fraction of substituents in this species is consistent with the fact that the substituted polymers already form poly-nuclear species at short length and prefer to build more nuclei instead of increasing the number of substituents in a single nucleus. In turn, this seems to favor a progressive increase in the polymer size along a straight line (the one passing through or close to the nuclei) rather than isotropically, a fact that accounts for the smaller increase in $\sqrt{\langle R_g^2 \rangle}$ for this species with respect to the ones with weaker HPS interactions amd smaller x_s.

4. Conclusions

In this work, we have presented the results of a theoretical study attempting to provide an answer to the experimentally relevant question: "how does the structure of a soluble polymer change upon varying the number and nature of hydrophobic pendants covalently–linked to the chain? ". Given the high relevance of this question to important fields such as protein folding and polymer science, it comes at no surprise that a lot of attention has already been paid to this problem, and semi-quantitative answers have been provided employing varying levels of sophistication in the polymer description. Apart from the useful insight on the structural properties of chain-like species in diluted solution or interacting with other molecules or solid surfaces (see for instance [24,25,42,44,45] and reference therein) and their dependency on the degree of hydrophobicity, the main message that can be extracted from these efforts is how incredibly complicated these systems are and how difficult it is to efficiently simulate their thermodynamics, let alone their dynamics.

In this respect, our work makes a very first step in filling some of the information gaps left open by previous studies, which have mainly focused on short to medium length chains ($N \leq 100$) and high fractional loads ($x_s > 0.5$) of hydrophobic substituents. For these species, one would *a priori* expect a compact hydrophobic core surrounded by very short chain loops whenever the temperature is sufficiently low (or the substituent interaction sufficiently high) to allow the core formation, an expectation that has been fulfilled by the computational results. Conversely, we have focused on studying model systems mimicking the properties of water soluble polymers ($N = 92$, 184 and 368) carrying a smaller number of hydrophobic pendants ($0 \leq x_s \leq 0.11$), with an emphasis on the analysis of the changes induced in their structural properties as a function of N, x_s and the strength of the hydrophobic interaction V_0. The ranges of parameters chosen for our models are consistent with species recently investigated or synthesized.

Perhaps not surprisingly, our results indicate that the chains acquire a more compact and less fluctuating structure (see Fig. 4) upon increasing x_s and the V_0. More interesting is the fact that the model systems may form more than one compact cluster of pendants, which are surrounded by chain loops and connected by means of short monomer chains. Although this finding may in principle be explained by invoking the semi-flexible nature of the chain and the monomer excluded volume effect, at the moment it is not clear what is the role played by the volume and flexibility of the pendants as well as by the entropy of the chain in modifying the free energy landscape. Given the general interest in preparing nano-species with controllable and tunable structures, more work appears to be warranted in order to extract general conclusions on the dependency of the free energy surface for this family of systems on the structural details of the chains. This will be the focus of future investigations in our laboratories.

As for the original motivation for the present study, we notice that the increasingly more compact structure as function of x_s and V_0 indicates a strong reduction in the system entropy at the level of a single species in solution, and the formation of closely packed hydrophobic nuclei shielded by chain loops. The net effect of this is a decrease in the exposure of the hydrophobic species to the local environment, which may in turn limit the attachment from enzymes and the release of the active molecule from the polymeric scaffold. From our calculations, this scenario begins to appear already for a 5% fractional load and for a strength of hydrophobic interaction which is afforded by systems such as bicyclooctane and adamantane [35]. Besides, the lower entropy afforded by a compact polymer-hydrophobic molecule conjugate in solution would be expected to reduce the driving force toward its solubilization and it may also affect the free energy barrier that need to be surmounted to leave the solid and become fully dissolved.

In concluding our discussion, we feel it is important to draw an interesting parallel between our simulation results and the nucleation phenomenon. In the latter, the external variable that kicks off the onset and defines the speed of nucleation (i.e. the aggregation

of monomers to form first clusters and subsequently nano-particles) is the supersaturation ratio, whose logarithm is proportional to the difference in chemical potential between monomers in a supersaturated system and its equilibrated counterpart. Such a difference in the chemical potential between two "phases" can be modulated, either increasing the concentration of the condensing species (in our case, the fraction of pendants x_s) or increasing the effective inter-particle interaction (i.e. increasing V_0), which in a condensing system may be induced by modifying the environment (e.g. using a different solvent). In both cases, the net outcome is to drive the system over the free energy barrier that separates the metastable state from the equilibrium one and to force nucleation. For the systems under investigation, however, the situation is made more complicated by monomers being tethered to a chain. The latter affects both the substituent motion, thus reducing the entropy of the dissociated state, and the minimum free energy structures due to the internal strain. The possible competition or synergy between these two effects is clearly not trivial to predict, and it may give rise to interesting physical phenomena or to peculiarities in the structure of these systems. This, also, would be subject of a future investigation.

Acknowledgments

The Authors would like to acknowledge useful suggestions and a careful read by Dario Bressanini, Gabriele Morosi, Emanuele Curotto and Samuel L. Stone.

References

[1] Ringsdorf H. J Polym Sci Polymer Symp 1975;51:135.
[2] Duncan R. Nat Rev Drug Discov 2003;2:347.
[3] Liong M, Lu J, Kovochich M, Xia T, Ruehm SG, Nel AE, et al. ACS Nano 2008;2:889.
[4] McCarthy JR, Weissleder R. Adv Drug Deliv Rev 2008;60:1241.
[5] Nasongkla N, Bey E, Ren JM, Ai H, Khemtong C, Guthi JS, et al. Nano Lett 2006;6:2427.
[6] Matsumura Y, Maeda H. Cancer Res 1986;6:6387.
[7] Weissleder R, Pittet MJ. Nature 2008;452:580.
[8] Kobayashi H, Kawamoto S, Star RA, Waldmann TA, Tagaya Y, Brechbiel MW. Cancer Res 2003;63:271.
[9] Lu ZR. Pharm Res 2007;24:1170.
[10] Hamoudeh M, Kamleh MA, Diab R, Fessi H. Adv Drug Deliv Rev 2008;60:1329.
[11] Rabin O, Manuel Perez J, Grimm J, Wojtkiewicz G, Weissleder R. Nat Mater 2006;5:118.
[12] Searle F, Gac-Breton S, Keane R, Dimitrijevic S, Brocchini S, Duncan R. Bioconjugate Chem. 2001;12:711.
[13] Keane R, Gac-Breton S, Searle F, R. Duncan. J. Pharm. Pharmacol 2000;52 (Suppl.):52.
[14] Greco F, Vicent MJ, Gee S, Jones AT, Gee J, Nicholson RI, et al. J Controlled Release 2006;117:29.
[15] Chen W-H, Liaw D-J, Wang K-L, Lee K-R, Lai J-Y. Polymer 2009;50:5211.
[16] Bohdanecky M, Bazilova H, Kopecek J. Eur Polym J 1974;10:405.
[17] Ulbrich K, Konak C, Tuzar Z, Kopecek J. Makromol Chem 1987;188:1261.
[18] Mendichi R, Rizzo V, Gigli M, Schieroni Giacometti A. J Liq Chromatogr. Relat. Technol 1996;19:1591.
[19] Shiah JG, Konak C, Spikes JD, Kopecek J. J Phys Chem 1997;101:6803.
[20] Mendichi R, Rizzo V, Gigli M. Bioconjugate Chem 2002;13:1253.
[21] Mendichi R, Rizzo V, Gigli M, Schieroni AGiacometti. J Appl Polym Sci 1998;70:3.
[22] Griffiths PC, Khayat Z, Tse S, Heenan RK, King SM, Duncan R. Biomacromolecules 2007;8:1004.
[23] Paul A, Vicent MJ, Duncan R. Biomacromolecules 2007;8:1573.
[24] Bachmann Michael, Handan Ark imathn, Wolfhard Janke. Phys Rev E 2005;71:031906.
[25] Bachmann Michael, Wolfhard Janke. Phys. Rev. Lett. 2003;91:208105.
[26] Higuchi Yuji, Sakaue Takahiro, Yoshikawa Kenichi. Chem Phys Lett 2008;461:42.
[27] Hu Dehong, Yu Ji, Wong Kim, Bagchi Biman, Rossky Peter J, Barbara Paul F. Nature 2000;405:1030.
[28] Reith Dirk, Müller Beate, Müller-Plathe Florian, Wiegandb Simone. J Chem Phys 2002;116:9100.
[29] Ghosh Tuhin, Kalra Amrit, Garde Shekhar. J Phys Chem B 2005;109:642.
[30] Hotta Takeshi, Kimura Akihiro, Sasai Masaki. J Phys Chem B 2005;109: 18600.
[31] Thomas Andrew S, Elcock Adrian H. J Phys Chem B 2007;129:14887.
[32] Dang Liem X. J Chem Phys 1994;100:9032.
[33] Setny Piotr. J Chem Phys 2007;127:054505.
[34] Zou Lizhuang, Yang Guanying, Han Buxing, Liu Ruilin, Yan Haike. Sci China Ser B: Chem 1999;42:225.
[35] Makowski Mariusz, Czaplewski Cezary, Liwo Adam, Scheraga Harold A. J Phys Chem B 2010;114:993.
[36] Metropolis N, Rosenbluth AW, Rosenbluth MN, Teller AH, Teller E. J Chem Phys 1953;21:1087.
[37] Betancourt MR, Chem J. Phys 2005;123:174905.
[38] Swendsen Robert H, Wang Jian-Sheng. Phys Rev Lett 1986;57:2607.
[39] Calvo F, Chem J. Phys 2005;123:124106.
[40] Zheng Lianqing, Luo Sheng-Nian, Thompson Donald L. J Chem Phys 2006;124:154504.
[41] Zhou Yaoqi, Karplus Martin, Wichert John M, Hall Carol K. J Chem Phys 1997;107:10691.
[42] Wüst Thomas, Landau David P. Phys Rev Lett 2009;102:178101.
[43] Bachmann M, Janke W. J Chem Phys 2004;120:6779.
[44] Bachmann Michael, Wolfhard Janke. Phys Rev E 2006;73:020901.
[45] Paul W, Strauch T, Rampf F, Binder K. Phys Rev E 2007;75:060801.